Published online 27 March 2017

Nucleic Acids Research, 2017, Vol. 45, No. 11 ***6321–6333***
doi: 10.1093/nar/gkx208

Heat shock factor 1 promotes TERRA transcription and telomere protection upon heat stress

Sivan Koskas[1], Anabelle Decottignies[2], Solenne Dufour[1], Mylène Pezet[1], André Verdel[1], Claire Vourc'h[1,*] and Virginie Faure[1,*]

[1]University Grenoble Alpes, INSERM U1209, CNRS UMR 5309, Institute for Advanced Biosciences, 38042 Grenoble Cedex 9, France and [2]De Duve Institute and Catholic University of Louvain, GEPI, 1200 Brussels, Belgium

Received August 09, 2016; Revised March 16, 2017; Editorial Decision March 19, 2017; Accepted March 20, 2017

ABSTRACT

In response to metabolic or environmental stress, cells activate powerful defense mechanisms to prevent the formation and accumulation of toxic protein aggregates. The main orchestrator of this cellular response is HSF1 (heat shock factor 1), a transcription factor involved in the up-regulation of protein-coding genes with protective roles. It has become very clear that HSF1 has a broader function than initially expected. Indeed, our previous work demonstrated that, upon stress, HSF1 activates the transcription of a non-coding RNA, named Satellite III, at pericentromeric heterochromatin. Here, we observe that the function of HSF1 extends to telomeres and identify subtelomeric DNA as a new genomic target of HSF1. We show that the binding of HSF1 to subtelomeric regions plays an essential role in the upregulation of non-coding TElomeric Repeat containing RNA (TERRA) transcription upon heat shock. Importantly, our data show that telomere integrity is impacted by heat shock and that telomeric DNA damages are markedly enhanced in HSF1 deficient cells. Altogether, our findings reveal a new direct and essential function of HSF1 in the transcriptional activation of TERRA and in telomere protection upon stress.

INTRODUCTION

Upon proteotoxic stress exposure, cells activate an essential and well-conserved defense mechanism named the proteotoxic cell response aiming at protecting cells from stress-induced damages. Among the large variety of stimuli capable of eliciting this cellular response, hyperthermia is considered as the founding and preeminent cellular stress (1,2). It induces transcriptional changes associated with genome-wide chromatin remodeling and also activates DNA damage response pathways (DDR), mostly due to its impact on proteins involved in DNA replication, chromosome segregation or DNA repair.

Heat shock factor 1 (HSF1), also identified as a tumor-promoting factor, is a key transcription factor of the heat shock response (HSR). In physiological conditions, HSF1 is in a complex with other proteins in a monomeric inactive state. Upon stress, HSF1 undergoes a multistep activation process involving post-translational modifications, nuclear localization and trimerization. Active HSF1 binds to specific heat shock elements (HSEs) present within gene promoters. A large number of HSF1 targets have been identified including the hsp genes encoding heat shock proteins (HSPs) (3). HSPs play important roles in both protein protection and protein homeostasis. In human stressed cells, HSF1 also triggers the transcriptional activation of pericentric heterochromatin. HSF1 binding to pericentric satellite III (Sat III) repetitive sequences, primarily at the 9q12 locus, results in the formation of HSF1 nuclear foci called nuclear stress bodies (nSBs). nSBs represent active transcription sites of sat III sequences into long non-coding Sat III RNA (4–6). The role of SatIII transcription and Sat III transcripts is still unclear. Interestingly, more recently, heat shock (HS) was also found to trigger an accumulation of long non-coding RNA of telomeric origin (7–9).

Telomeres belong to constitutive heterochromatin and play a vitally important part in chromosome integrity and stability. They protect the end of linear chromosomes from degradation and from recognition as double-strand breaks by the DNA damage repair machinery. Telomeres are protected by a shelterin complex, essential for their structural maintenance and stability (10). This complex involves six proteins among which the double strand specific factor TRF2 (telomeric repeat factor 2) that has emerged as a key player in telomere protection. TRF2 specifically prevents telomeres recognition as DNA double strand breaks by repressing the activation of the ATM (ataxia telangiectasia mutated) kinase signaling pathway, and it also protects

*To whom correspondence should be addressed. Tel: +33 476 549 446; Fax: +33 476 549 425; Email: virginie.faure@univ-grenoble-alpes.fr
Correspondence may also be addressed to Claire Vourc'h. Tel: +33 476 549 470; Fax: +33 476 549 425; Email: claire.vourch@univ-grenoble-alpes.fr

telomeres from end-fusions elicited by the non homologous end-joining pathway (11).

Telomeres are transcribed by RNA polymerase II (RNAPII), into heterogeneous long non-coding RNA called TERRA (telomeric repeat containing RNA) (7,12). TERRA transcription is initiated within chomosome-specific subtelomeric regions, ending in the telomeric tract. Consequently, individual TERRA sequences vary between chromosomes. TERRA transcription start sites are located within CpG islands at a subset of telomeres, supporting the existence of subtelomeric promoters driving TERRA transcription (13). Different repressors of TERRA transcription have been identified including DNA methyltransferases like DNMT1 and DNMT3b (13,14), or histone methyltransferases like SUV39H1 combined with the heterochromatin protein 1 α (HP1α) (7,15). TERRA is also upregulated by the mixed lineage leukemia (MLL) protein after induction of telomere uncapping (16). Different telomeric functions have been assigned to TERRA transcripts including a role in telomerase regulation (7,17–19), in telomere stability and replication (15,20,21) and in the telomeric DNA damage response (11).

Telomeric integrity and transcription are both impacted by heat stress. In yeast, long heat exposure shortens telomeres after a hundred generations (9) and alters telomere length distribution and subtelomeric methylation status in human endothelial cells (22). Likewise, Martinez-Guitarte *et al.* have provided the first data showing an increased transcription at telomeres upon HS in *Chironomus thummi*, with a decondensation of telomeric heterochromatin correlating with RNA polymerase II (RNAPII) and histone H4 acetylation accumulation at these regions (23). In addition, HS has been found to promote TERRA accumulation in both mouse (7) and human (8) cells.

While a direct implication of HSF1 in stress-induced transcriptional activation of human pericentric heterochromatic regions has already been demonstrated, its implication at other heterochromatin regions is unknown. Moreover, the mechanisms by which telomeres and telomeric transcripts are impacted by stress in mammals are still unknown. Here, we show that telomeres are new and important targets of HSF1, and identify HSF1 as the first transcription factor involved in TERRA up-regulation in response to stress. These findings highlight a new original role of HSF1 in the maintenance of telomeres integrity in heat shocked cells.

MATERIALS AND METHODS

Cell culture and heat stress treatments

HeLa wild type (WT) cells are derived from cervical cancer cells. HFF2 cells, are human foreskin fibroblast transfected with the catalytic subunit of the telomerase TERT. HT1080 cells are fibrosarcoma cells from ATCC. All cell lines were cultured in Dulbecco's modified Eagle's medium (DMEM) supplemented with 10% decomplemented fetal bovine serum, 2% L-glutamine (4 mM) and 100 units per ml penicillin and 100 mg/ml streptomycin and grown in 5% CO_2 atmosphere at 37°C. Stable HSF1 knock down (HSF1 KD) HeLa cells containing stable expression of shRNA against HSF1 were grown in HeLa WT medium supplemented with Geneticine antibiotic at 0.4% final concentration. HS was performed in a water bath for 1 h at 43°C followed or not by a recovery period at 37°C.

Chromatin immuno-precipitation (ChIP)

For IgG, RNAPII, TRF2 and γ-H2AX ChIP analysis, cells were cross-linked with 1% formaldehyde at room temperature (RT) for 10 min before the addition of 125 mM glycine (Sigma) for 5 min. After washing, cell nuclei were isolated by suspending cells into cytosol lysis buffer (10 mM HEPES (pH 6.5), 0.25% Triton-x, 0.5 mM EGTA, 10 mM EDTA) at 4°C for 5 min. Nuclei were resuspended in nuclei lysis buffer before sonication at 4°C for 19 min with a BioRuptor sonicator (Diagenode) to obtain fragments between 200 and 800 bp. Samples were incubated overnight with the antibodies listed in Supplementary Table S1 and immunoprecipitated using the OneDay ChIP kit (Diagenode), following the manufacturer instructions. Immunoprecipitated DNA was analyzed either by qPCR, using primers listed in Table Supplementary Table S2, or by DNA dot-blot, using a Telo $(CCCTAA)_4$ probe labeled with [γ-32P]ATP (PerkinElmer) using T4 polynucleotide kinase (New England Biolabs). For RNAPII ChIP, three couples of primers were designed for each chromosome arm. Indeed, it has been shown that elongating RNAPII binds as a diffuse peak most frequently at positions close to *TTAGGG* repeats and at regions overlapping CpG islands (24). For dot blot, alpha satellite sequences, used as controls, were labeled by the Megaprime DNA Labeling System (GE Healthcare) and [α-32P]dCTP (PerkinElmer). Images were captured with a Phosphorimager (BioRad) and signals were quantified using the 'Quantity one' software. For TRF2 ChIP analysis, cells were submitted to a kinetic of HS between 5 and 60 min exposure. For HSF1 ChIP analysis, we performed the method described previously (25).

Simultaneous immunofluorescence (IF), DNA or RNA fluorescence *in situ* hybridization (FISH)

Cells were grown on coverslips and heat-shocked or not as described above. Briefly, cytosol was preextracted with a permeabilization buffer (20 mM Tris–HCl (pH 8), 50 mM NaCl, 3 mM $MgCl_2$, 300 mM sucrose, 0.5% Triton X-100) then all cells were fixed in 4% paraformaldehyde in PBS for 15 min, washed thoroughly and nuclei incubated with a permeabilization buffer. Labeling of HSF1, γ-H2AX and TRF2 were first performed on formaldehyde-fixed cells. The characteristics of the antibodies used are listed in Supplementary Table S1. After detection with the secondary antibody, cells were fixed again in 4% formaldehyde and processed for DNA FISH. Briefly prior to *in situ* hybridization, nuclei were successively dehydrated in 70%, 90% and 100% EtOH. For telomeric DNA staining, cells were incubated for 3 min at 80°C with 2 ng/μl of PNA TelC-Cy3 (polynucleid acid telomeric C-rich probe coupled with a cyanine 3 fluorochrome from Eurogentec) diluted in hybridization mix (70% formamide/Tris 20 mM, 0.5% blocking reagent (Roche), 5% Mg buffer), followed by 1 h hybridization at RT. Finally, cells were washed in formamide and in Tris–

Tween 0.08%. For TERRA detection, cells were first permeabilized with CSK buffer (10 mM Pipes, pH 7.0, 100 mM NaCl, 300 mM sucrose, 3 mM $MgCl_2$, 0.5% Triton X-100, 10 mM ribonucleoside vanadyl complex (New England Biolabs)). TERRA FISH was performed as described previously (15), except for hybridization that was performed at 37°C for 2 h with 400 nM PNA C-rich (Eurogentec), in 50% deionized formamide, 10% dextran sulfate (Millipore), 2XSSC, 2 mg ml^{-1} BSA and 10 mM RVC (New England Biolabs). Cells were rinsed with 0.1× SSC at 60°C and with 2× SSC at room temperature. DNA was counterstained with 250 ng/ml 4′,6-diamidino-phenylindole (DAPI). Slides were mounted with a Dako fluorescent mounting medium (Invitrogen).

Image acquisition and measurement

Microscopy experiments were performed on a structured illumination (pseudo-confocal) imaging system (ApoTome-AxioImager Z1, Zeiss) equipped with a monochromatic CCD camera (AxioCam MRm, Zeiss) and controlled by the AxioVision software. A minimum of 10 z-planes were acquired with a 63× oil immersion objective (Plan-Apochromat NA 1,4 Oil, Ph3, WD 190 nm) to constitute a 3D image. Z-stacks images (1388 × 1040 pixels per frame using a 12-bit pixel depth for each channel at a constant voxel size of 0.1 μm × 0.1 μm × 0.24 μm) were acquired. Segmentation and 3D measurements between objects corresponding to telomeres and γ-H2AX or TRF2 but also to TERRA foci were performed with the Volocity software (PerkinElmer). The background level was obtained by measuring the mean intensity of each stain outside the cells. Objects were segmented out from the background with a minimal intensity for each channel applied thereafter for all images. Object based colocalization was then analyzed on thresholded images from the red/green intensities by calculating Manders' coefficients based on the co-occurrence of the two probes at the same voxel location thus representing the fractional overlap. A Mander's coefficient value >0.5 was considered as a positive colocalization. The 3D point spread functions were the same for different excitation and emission wavelengths and there was no registration shift between images. This checking was done through imaging 0.5 μm diameter multicolor fluorescent beads. No significative differences were observed in the X, Y or Z directions.

RT Q-PCR

Total RNA was extracted from Hela cells deficient or not for HSF1, using Trizol reagent (Sigma) in RNase free conditions. RNA was treated with DNase (Ambion) for 30 min at 37°C. 1 μg of RNA was reverse transcribed with equal amount of random hexamers and telomere specific $(CCCTAA)_5$ oligonucleotides using First-Strand cDNA Synthesis kit (Roche), according to the manufacturer's instructions. Controls without reverse transcriptase or RNA were performed. For quantification of TERRA transcripts at 2p, 3p, 14q and 10–18p subtelomeric regions and of Hsp70, SYBER green (master mix TAKARA) incorporation-based, real-time PCR analysis were performed using specific primers (see Supplementary Table S2). Q-PCR was performed on a LCR408 (Light-cycler ROCHE) machine.

RNA dot blot

10 μg of RNA resuspended in SSC and formaldehyde were denatured at 70°C and then dot-blotted on a positively charged nylon transfer membrane (GE Healthcare), and UV crosslinked with a UV-stratalinker (Stratagene). TERRA and U2 were detected using a $(CCCTAA)_5$ or a U2 specific oligonucleotide probe labeled with ^{32}P-γ-ATP by T4 polynucleotide kinase (NEB) and purified with illustra microspin G-25 columns (GE Healthcare). Hybridizations were performed using UltraHyb buffer (Ambion) for 16–18 h at 43°C or 50°C. Membranes were washed in 2× SSC/0.1% SDS for 10 min at room temperature and in 0.2× SSC/0.1% SDS for 20 min at 50°C. Blots were stripped for 10 min with 0.1× SSC, 40 mM Tris (pH 7.5), and 1% SDS buffer preheated at 80°C. When indicated, RNA samples were treated with RNaseA (Roche) at a final concentration of 100 μg/ml for 30–60 min at 37°C. Images were captured with a Phosphorimager (BioRad) and signals were quantified using 'Quantity one' software.

RNA stability

Stressed and unstressed WT and HSF1 KD cells were incubated with 1 μM of triptolide for 2–8 h. After RNA extraction with trizol agent, 3 μg of *S. pombe* RNA was added to each sample as an internal control for reverse-transcription efficiency. Total RNA was reverse-transcribed with a mix of telomeric and *S. Pombe* β-actin specific primers and random hexamer primer. TERRA from chromosomes 2p, 3p, 18q, 10p and 14q and U2 cDNA levels were quantified by q-PCR and normalized with *S. Pombe* β-actin cDNA levels used as a control.

Western blot analysis

HeLa WT and HSF1-KD cells were submitted to a kinetics of HS (5 min to 1 h at 43°C) or were submitted or not to a kinetics of recovery (2–6 h) following a 1 h HS. Cells were collected by a 5 min centrifugation at 2500 rpm, 4°C. Cell lysis was performed in NP40 buffer (Tris 20 mM (pH 7.5), NaCl 150 mM, EDTA 2 mM, NP40 1%) on ice and then cells were sonicated for 5 min (30 s ON, 30 s OFF) at 4°C. Protein extracts were obtained after 1 min centrifugation at 14 000 rpm at 4°C. Total protein extracts were quantified by spectrophotometry using a Bradford assay. Equal amounts (25–50 ug) of whole protein extracts were loaded and separated on 6%, 8% or 15% Acrylamide gels. Primary antibodies against HSF1, TRF2 and γ-H2AX listed in Supplementary Table S1 were used and diluted in PBS 1×, BSA 1%. Membranes were washed in PBS 1× Tween 0.1% (except for HSF1 staining wash with PBS 1× NaCl 0.1 M) and then incubated with secondary antibodies anti-rabbit or anti-mouse IgG linked with a fluorochrome. For loading controls, mouse polyclonal anti-tubulin antibodies were used. Target protein signal was obtained using ECL (GE Healthcare) and revealed using ChemiDoc MP System (Bio Rad). Band intensities were quantified using ImageJ software.

In sillico analysis

Bioinformatics databases were explored within 5 kb of subtelomeric regions (vader.wistar.upenn.edu/humansubtel) (26). Identification of CpG dinucleotide contents and a prediction of CpG islands, were done with the CpGPlot/CpGReport at the European molecular biology open software suite program (EMBOSS: http://www.ebi.ac.uk/Tools/emboss/cpgplot/).

RESULTS

TERRA accumulation upon HS requires HSF1

To assess the possible role of HSF1 in TERRA upregulation, we isolated total RNA fractions from unstressed and stressed HSF1 WT and KD HeLa cells. Hyperphosphorylated active form of HSF1, characterized by a lower electrophoretic mobility, was only detected in WT heat-shocked cells (Figure 1A). No major difference in the growth curves of WT and HSF1 KD HeLa cell type was observed. (Supplementary Figure S1). A quantification of TERRA was performed by RNA dot blot with a C-rich telomeric probe (Figure 1B). A 1.8-fold heat-induced increase of TERRA accumulation was observed in WT cells but not in stable HSF1 KD cells (Figure 1C) or in transient HSF1 KD cells (Supplementary Figure S2). Stress-induced accumulation of TERRA was specific and not observed for the *U2* housekeeping gene also used as a control. Similarly, HSF1-dependent upregulation of TERRA was observed in normal and tumorigenic fibroblasts (Supplementary Figure S3).

The intranuclear distribution of TERRA was further analyzed by RNA Fluorescence *in situ* Hybridization (RNA FISH) with a TERRA-specific probe (Figure 1D). In both unstressed and stressed HeLa cells, TERRA was present as nuclear discrete foci while, as expected, no TERRA was detected in cells pre-treated with RNase A. The volume of TERRA foci was then individually quantified from 3D reconstituted images using volocity software (Figure 1E). After a 1 h HS, a 2.6-fold increase in the volume of TERRA foci was only observed in stressed WT cells relative to unstressed cells, in agreement with a heat-induced TERRA accumulation in these cells. In contrast, no variation of TERRA volume was observed in HSF1 KD cells after HS. Interestingly, a 1.5 times decrease in the total number of TERRA foci was observed in heat-shocked WT cells, either suggesting a down regulation of TERRA expression at a subset of specific telomeres or an intranuclear redistribution of TERRA transcripts (Figure 1F). Indeed, no variation in the number of telomeres per nucleus was observed in unstressed and stressed WT and HSF1 KD cells (Figure 1G). In addition, after cell fractionation, we have shown that more nuclear TERRA was present in chromatin-bound fraction after heat shock (Supplementary Figure S4). Altogether, our RNA FISH and dot blot experiments indicate that in heat-shocked cells, TERRA accumulates within nuclear foci, in a HSF1 dependent-manner.

HSF1-dependent accumulation of TERRA is chromosome-specific

Upon stress, HSF1 binds to the repetitive pentameric sequences nGAAn, termed HSEs, present at promoters of HS genes (27–29). The number of HSEs and their sequence homology with the canonical HSE motif is thought to account for differences in HSF1 affinity for its targets (30,31). To further examine the mechanisms underlying HSF1-dependent accumulation of TERRA at telomeres, we first screened human subtelomeres for the presence of HSEs using an *in silico* approach. The presence of CpG dinucleotides elements, a characteristic of putative TERRA transcriptional start sites, was also examined. Our analysis revealed the existence of putative HSEs in 40% of all subtelomeres, within 5 kb upstream of the telomeric repeats (Figure 2A). In addition, CpG islands were also detected in 25% of HSE containing subtelomeric regions. These findings suggest that HSF1 only binds to a subset of subtelomeric regions.

A chromosome specific analysis of TERRA expression revealed a 2 to 3-fold accumulation of TERRA at telomeres containing subtelomeric HSEs by RT-qPCR on cells submitted to HS exposures of 5 min to 1 h (Figure 2B). The kinetics of HSF1 activation was monitored by western blot analysis (Figure 2C). Five different subtelomeric regions were examined, either displaying both HSEs and CpG islands (3p and 10p–18p) or no HSE (2p, 14q) (Figure 2D). Accordingly, the level of TERRA enrichment determined upon HS was higher in the case of HSE containing telomeres than when determined with a global, non-chromosome-specific approach (Figures 1C and 2B). The chromosome-specific pattern in heat-induced TERRA upregulation was confirmed on a larger set of telomeric regions (Supplementary Figure S5).

To further test the existence of a restricted binding capacity of HSF1 at HSE-containing subtelomeric regions, we then evaluated HSF1 binding to human subtelomeric regions by ChIP during the same kinetics of HS. The hsp70 promoter gene was used as a positive control. As shown in Figure 2E, a specific HSF1 enrichment was only observed at subtelomeric regions containing at least one HSE, supporting a chromosome-specific binding capacity of HSF1 at subtelomeric regions upon HS. Additionally, the kinetics of HSF1 binding to subtelomeric regions was slightly delayed (HSF1 enrichment is observed after 30 min HS) when compared to the well-characterized Hsp70 HSF1 target gene (HSF1 enrichment observed after 5 min of HS) possibly revealing differences of binding affinities or mechanisms for HSF1 between Hsp70 gene and subtelomeric regions. HSF1 binding to telomeres was also confirmed by *in situ* immuno-DNA FISH approaches which show a co-detection of both telomeres and HSF1 only upon heat shock conditions (Supplementary Figure S6).

Of note, the kinetics of HSF1 enrichment at subtelomeric regions slightly preceded that of TERRA accumulation (Figure 2B–E). Indeed, while HSF1 enrichment at HSE containing subtelomeres was already detected after 30 min of continuous HS, TERRA up-regulation was only detected 45 min after HS. Collectively, our findings strongly suggest that the heat-induced accumulation of TERRA is telomere-

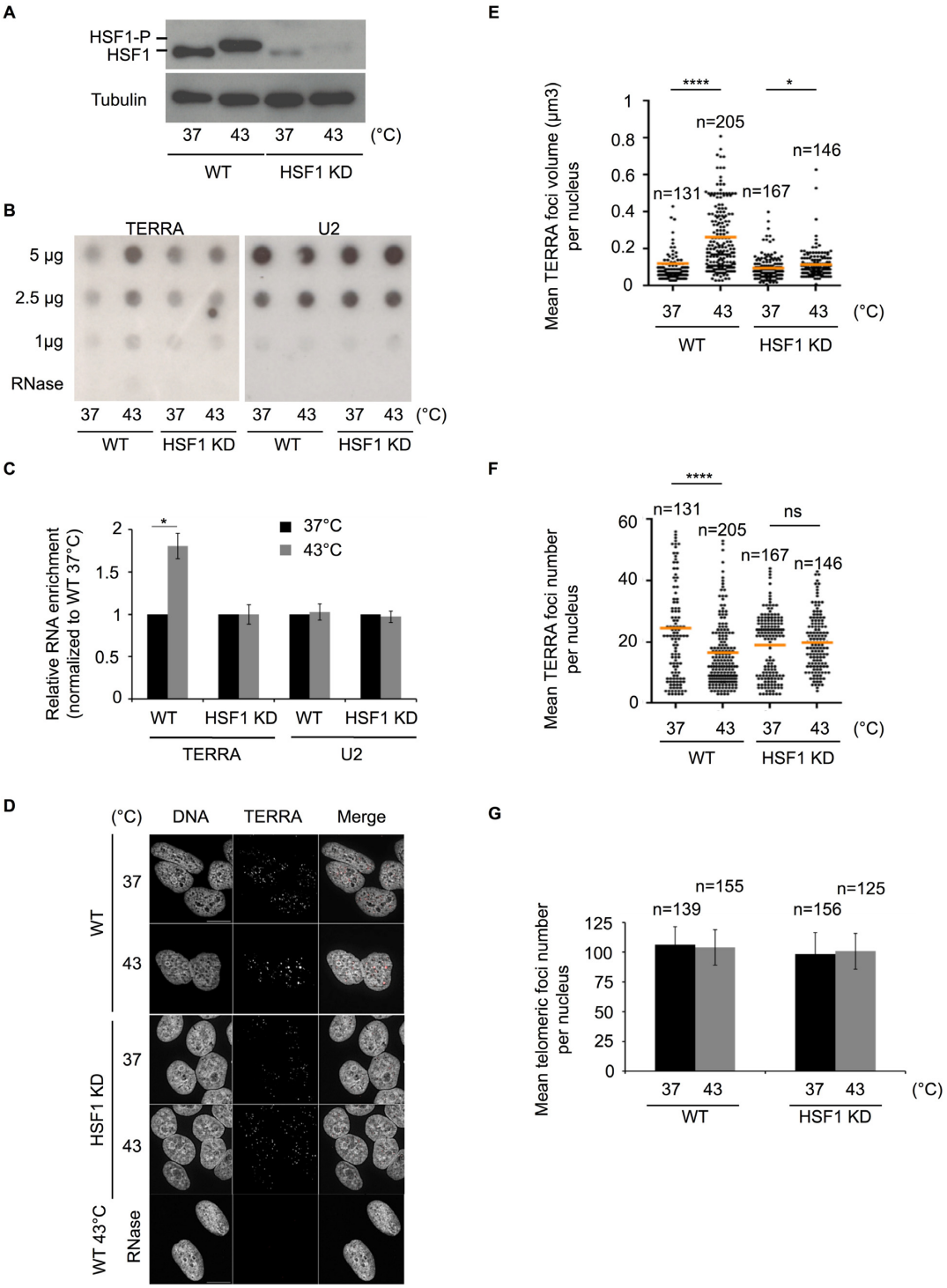

Figure 1. TERRA accumulation requires HSF1 upon heat shock. (**A**) Western blot analysis of HSF1 WT and KD unstressed and stressed cells. Tubulin is shown as a loading control. (**B**) Dot blot analysis of TERRA. Total RNA was extracted from WT and HSF1 KD cells before and after HS and treated with DNAse. Various amount of total RNA fractions were subjected to RNA dot blot analysis using a radiolabelled TERRA probe. RNA were treated with RNase in parallel.The same blot was also hybridized after staining with a control probe specific for U2 transcripts. (**C**) Quantification of TERRA and U2 levels in WT and HSF1 KD cells before and after HS normalized with 37°C conditions. Standard deviation (SD) was calculated from 3 independent experiments. *P*-value = 0.0213 (**D**) Representative confocal images of FISH analyses of TERRA expression in WT and HSF1 KD cells before and after HS. RNase treatment induces an elimination of TERRA signal. Scale bar: 10 µm. (**E**) 3D quantification analysis of mean TERRA foci volume in the different conditions tested by RNA FISH using volocity software. The *P*-values calculated by unpaired Student's *t*-test with Welch's corrections at 37°C and at 43°C for WT and HSF1 KD cells are respectively $P < 0.0001$ and $P = 0.0224$. (**F**) 3D quantification analysis of mean TERRA foci number per nucleus in the same conditions than described above. The *P*-values calculated by unpaired Student's *t*-test with Welch's corrections at 37°C and at 43°C for WT and HSF1 KD cells are respectively $P < 0.0001$ and non significative. (**G**) Quantification of telomeric foci per nucleus by DNA FISH in WT and HSF1 KD cells before and after HS.

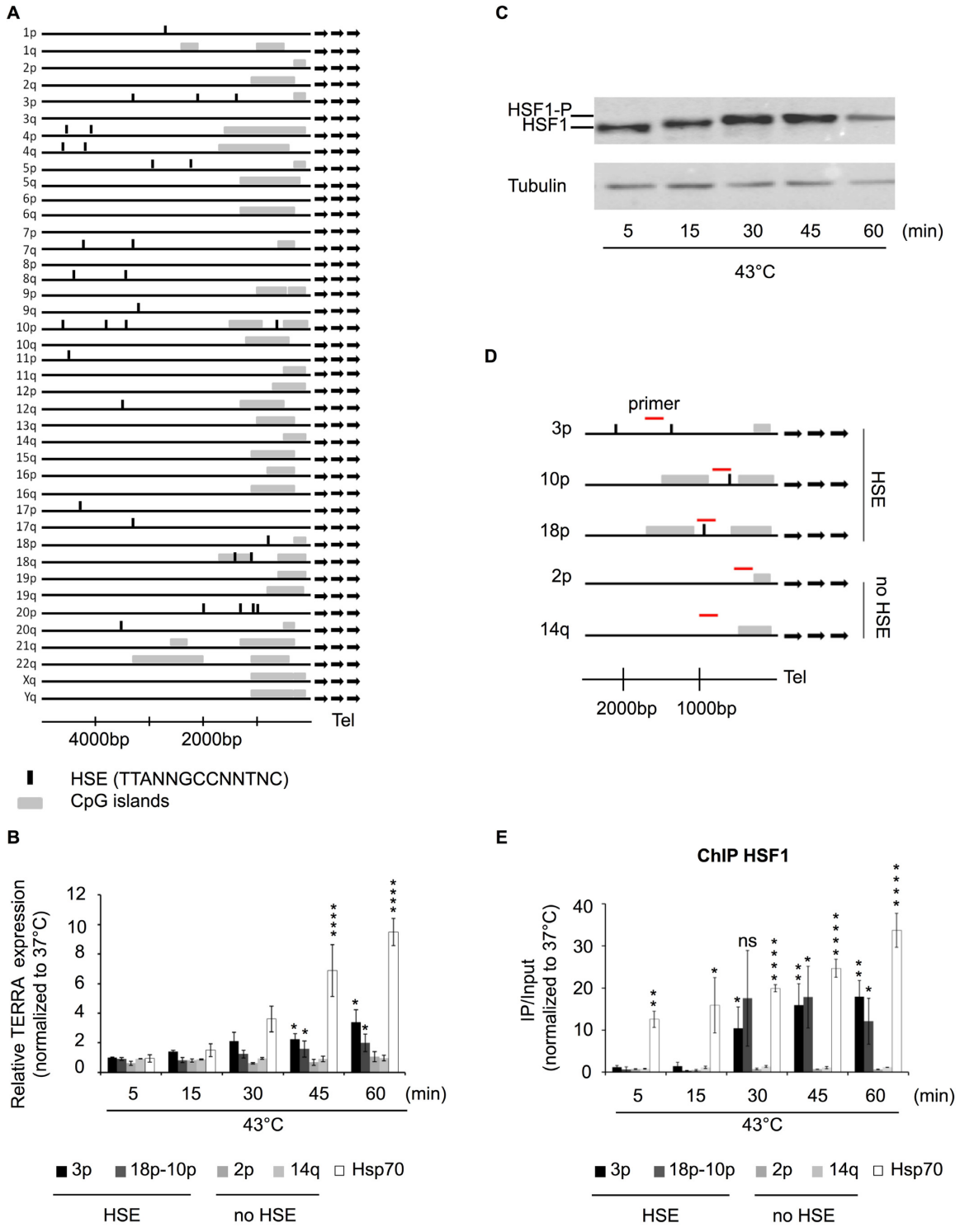

Figure 2. HSF1-dependent accumulation of TERRA is chromosome-specific. (**A**) Schematic diagram showing HSE binding sites and CpG islands positions as well as their distance from telomeres (Tel) on a large panel of human chromosomes. (**B**) TERRA transcripts from chromosomes 3p, 18p, 10p, 2p and 14q were quantified by RT-Q-PCR during the same kinetics of HS. Quantification of Hsp70 transcripts is used as a positive control. SD was calculated from two independent experiments. *P*-value was calculated by unpaired Student's *t*-test with Welch's corrections. For 3p, *P*-values are 0.0166 and 0.0443 at 45 and 60 min respectively. For 18p–10p, *P*-values are 0.0119 and 0.0197 at 45 and 60 min respectively. For hsp70, *P*-values are 0.001 and <0.0001 at 45 and 60 min respectively. (**C**) Western blot analysis of HSF1 in WT cells during the kinetics of HS. Tubulin is used as a loading control. (**D**) Positions of subtelomeric regions on chromosomes 3p, 18p, 10p, 2p and 14q up to 2500 bp from telomeres (Tel) (**E**) Quantification of HSF1 enrichment during HS kinetics at subtelomeres and at Hsp70 promoter regions determined by ChIP and q-PCR analysis. SD was calculated from three independent experiments. *P*-value was calculated by unpaired Student's *t*-test with Welch's corrections. For 3p, *P*-values are 0.034, 0.0075 and 0.0016 at 30, 45 and 60 min respectively. For 18p–10p, *P*-values are 0.0154, 0.0227 at 45 and 60 min respectively. For HSP70, *P*-values are 0.0005, 0.017 at 5 and 15 min respectively and <0.0001 for 30, 45 and 60 min.

specific and relies on the binding of HSF1 to HSEs at subtelomeric regions.

Heat-induced accumulation of TERRA relies on increased transcription rather than RNA stabilization

Despite strong evidence suggesting a direct role of HSF1 in the control of TERRA expression in heat-shocked cells, the possibility that TERRA accumulation may involve increased TERRA stability could not be formally excluded at that stage. To clarify this point, we monitored the impact of HSF1 activation on TERRA stability and RNAPII engagement at subtelomeric regions. To this end, WT and HSF1 KD cells were treated or not with triptolide, a potent inhibitor of RNAPII and submitted to a one-hour HS (experimental scheme shown in Supplementary Figure S7A). Chromosome-specific TERRA transcripts were then subsequently quantified by RT-qPCR at different time points of the recovery period (0–8 h). As shown in Figure 3A, no significant differences in TERRA stability was observed in WT and HSF1-deficient cells for chromosomes 14q, 18p–10p, 3p and 2p following HS. As expected, stress-induced TERRA upregulation was no more observed in cells treated with Triptolide (Supplementary Figure S7B and C).

Likewise, the evolution of RNAPII occupancy was performed by ChIP analysis, using an antibody directed against the elongating fraction of RNAPII (RNAPII-Ser2) (32,33). For each chromosome arm, three couples of primers (Figure 3B) were designed and tested. Heat-induced enrichment of elongating RNAPII at the pericentric region of chromosome 9 (SatIII) was used as a positive control. The specificity of RNAPII-Ser2 enrichment was assessed with an IgG control antibody (Supplementary Figure S8). Importantly, as shown in Figure 3C, a specific enrichment of RNAPII-Ser2 was exclusively observed at subtelomeric regions displaying HSEs and upon HS. In contrast, no enrichment of RNAPII-Ser2 was observed in HSF1 KD stressed cells. Altogether, our findings demonstrate that the heat-induced accumulation of TERRA relies on transcriptional activation.

Heat shock alters telomere capping and telomere integrity

Evidence exists that HS impacts on telomere length and induces modifications in nuclear TRF2 localization (9,22,34). Because TRF2 is a protein with an important role in telomere capping and integrity (11), we sought to further examine the impact of HS on telomeric protection and integrity. *In situ* approaches combining the detection of telomeric DNA by FISH and that of TRF2 by immunostaining were performed to evaluate the extent of telomere capping that corresponds to telomeric protection (Figure 4A). The minimal distances between TRF2 and telomere foci were estimated from reconstituted 3D fluorescence images. Consistent with published data (34), a partial dissociation of TRF2 from telomeres was observed upon HS (Figure 4B). In addition, a significant but less pronounced telomeric uncapping upon HS is observed in HSF1 KD cells. These results suggest that HS induces partial TRF2 dissociation. The specificity of the antibody against TRF2 was validated (Supplementary Figure S9). In parallel, the telomeric dissociation of TRF2 was also confirmed during a kinetics of HS exposure and quantified by ChIP analysis in WT and HSF1 KD cells (Figures 4C and D). Our results reveal a 50% decrease of TRF2 telomeric binding after only 5 min of stress exposure in these cells. TRF2 expression was not impacted by HS as shown by western blot analysis (Figure 4E and F).

Since, γ-H2AX is a well-known molecular marker of DNA damages, the number of γ-H2AX foci colocalizing with telomeres, also known as TIF (telomere dysfunction-induced foci), was then compared in unstressed and stressed HeLa cells. TIF were detected in wild type HeLa cells submitted to a 1 hour HS using an immunoFISH approach allowing a co-detection of γ-H2AX and telomeres (Figure 5A), and their quantification was determined from 3D fluorescence images. As shown in Figure 5B, a significant increase in the percentage of cells with at least five TIF was observed upon HS in WT cells, consistent with a harmful role of stress on telomere integrity. The impact of HS on TIF formation was also confirmed in two other cell lines (HT1080 and HFF2-TERT) (Supplementary Figure S10), clearly indicating that the impact of HS on telomeric integrity is a general mechanism.

HSF1 helps maintaining telomere integrity during HS

We next examined the role played by HSF1 in telomere protection against stress-induced DNA damages. The importance of HSF1 for telomere integrity was both determined by *in situ* (Figure 5A) and ChIP analyses (Figure 5C) on WT and HSF1 KD cells. The quantification of γ-H2AX enrichment at telomeres was first analyzed by immuno-FISH. A 2-fold increase in the percentage of cells with at least five TIFs was observed in heat-shocked cells in which HSF1 is stably (Figure 5B) or transiently knocked down (Supplementary Figure S11) when compared to heat-shocked WT cells, highlighting a critical role for HSF1 in telomere protection upon stress. In ChIP experiments, a 2-fold enrichment of telomeric γ-H2AX binding was also observed upon stress in HSF1 KD HeLa cells when compared to WT cells (Figure 5C and D). In addition, no γ-H2AX enrichment was detected at centromeric regions thus revealing the specificity of γ-H2AX enrichment at telomeres. Additionally, no global increase in the amount of nuclear γ-H2AX was observed upon stress in HSF1 KD cells when compared to WT HSF1 cells (Figure 5E and F), indicating that γ-H2AX enrichment observed at telomeres in HSF1 KD cells does not result from a higher global level of γ-H2AX in these cells.

Finally, HSF1 is not only involved in maintaining the balance between key cellular functions upon stress but is also critical in restoring these functions following stress exposure. To assess the impact of HSF1 KD on the kinetics of telomeric DNA damage repair during the recovery period from stress, the presence of TIF was quantified at different time points (from 1 hour to 6 hours) of the recovery period following a one hour heat shock. No impact of HSF1 on the speed of resolution of telomere damages was however observed (Supplementary Figure S12). Our findings thus reveal a new role for HSF1 in protecting telomere integrity upon stress.

DISCUSSION

Heat shock has a deleterious effect on telomere integrity. In

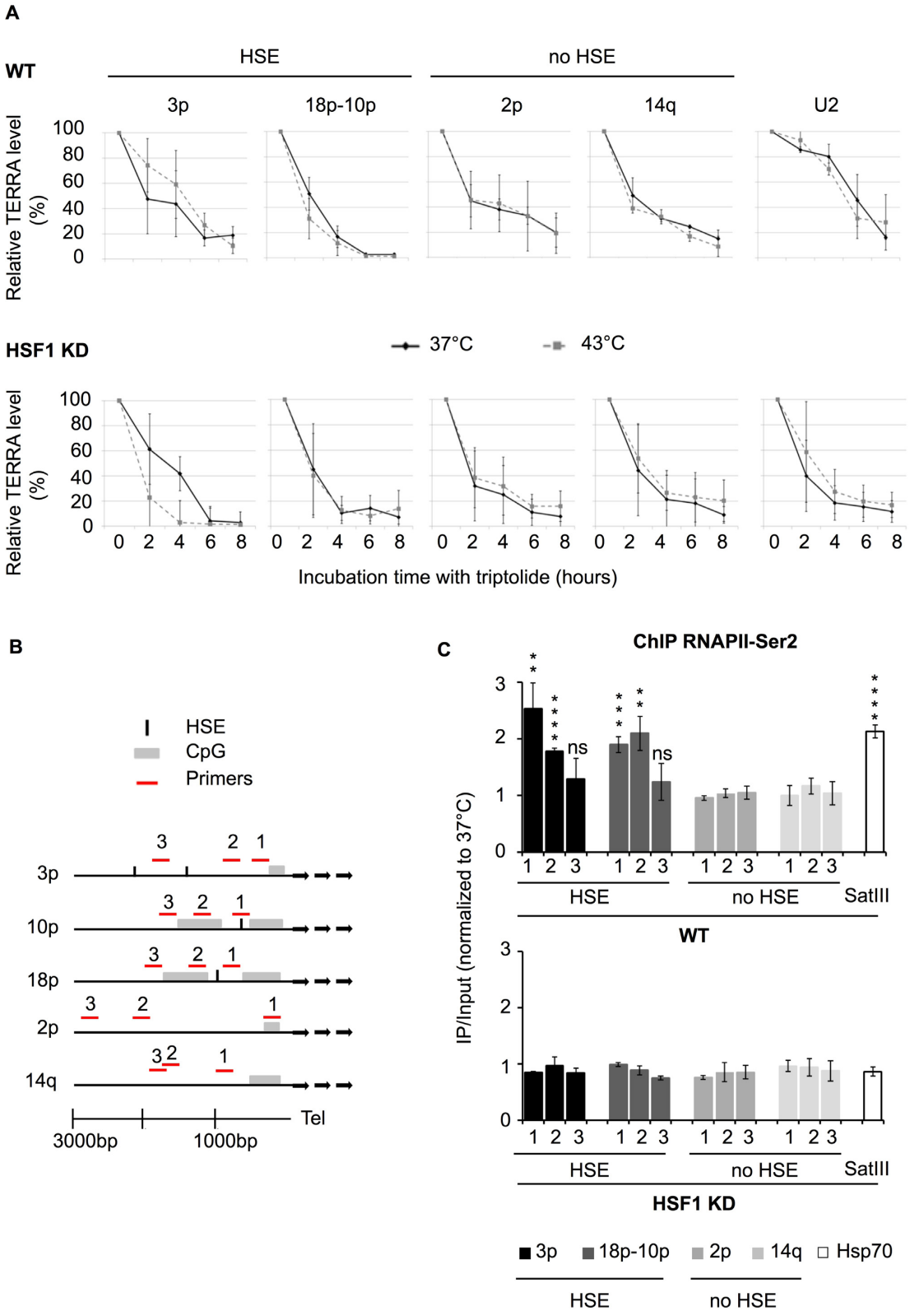

Figure 3. Heat-induced accumulation of TERRA relies on increased transcription rather than RNA stabilization. (**A**) TERRA encoded by chromosomes 3p, 18p, 10p, 2p, 14q and U2 transcripts were quantified, at 37°C and 43°C by qRT-PCR in WT and HSF1 KD cells. Results were normalized with an exogenously act1 cDNA added yeast RNA, and were depicted as percentages of the time point 0. SD was calculated from 3 independent experiments. (**B**) Positions of the primers selected for elongating RNAPII ChIP analysis on subtelomeric regions of chromosomes 3p, 18p, 10p, 2p, 14q up to 3000 bp from telomeres (Tel). (**C**) Relative enrichment of elongating RNAPII at subtelomeric regions of 3p, 18p, 10p, 2p, 14q and of the SatIII gene was quantified in stressed WT and HSF1 KD cells by q-PCR and normalized with both Input and values corresponding to 37°C conditions. SD is based on three independent experiments. *P*-value was calculated by unpaired Student's *t*-test with Welch's corrections. For 3p, *P*-values are 0.0041 and <0.0001 for V1 and V2 primers respectively. For 18p–10p, *P*-values are 0.0004 and 0.0031 for V1 and V2 primers respectively. For SatIII, *P*-value is <0.001.

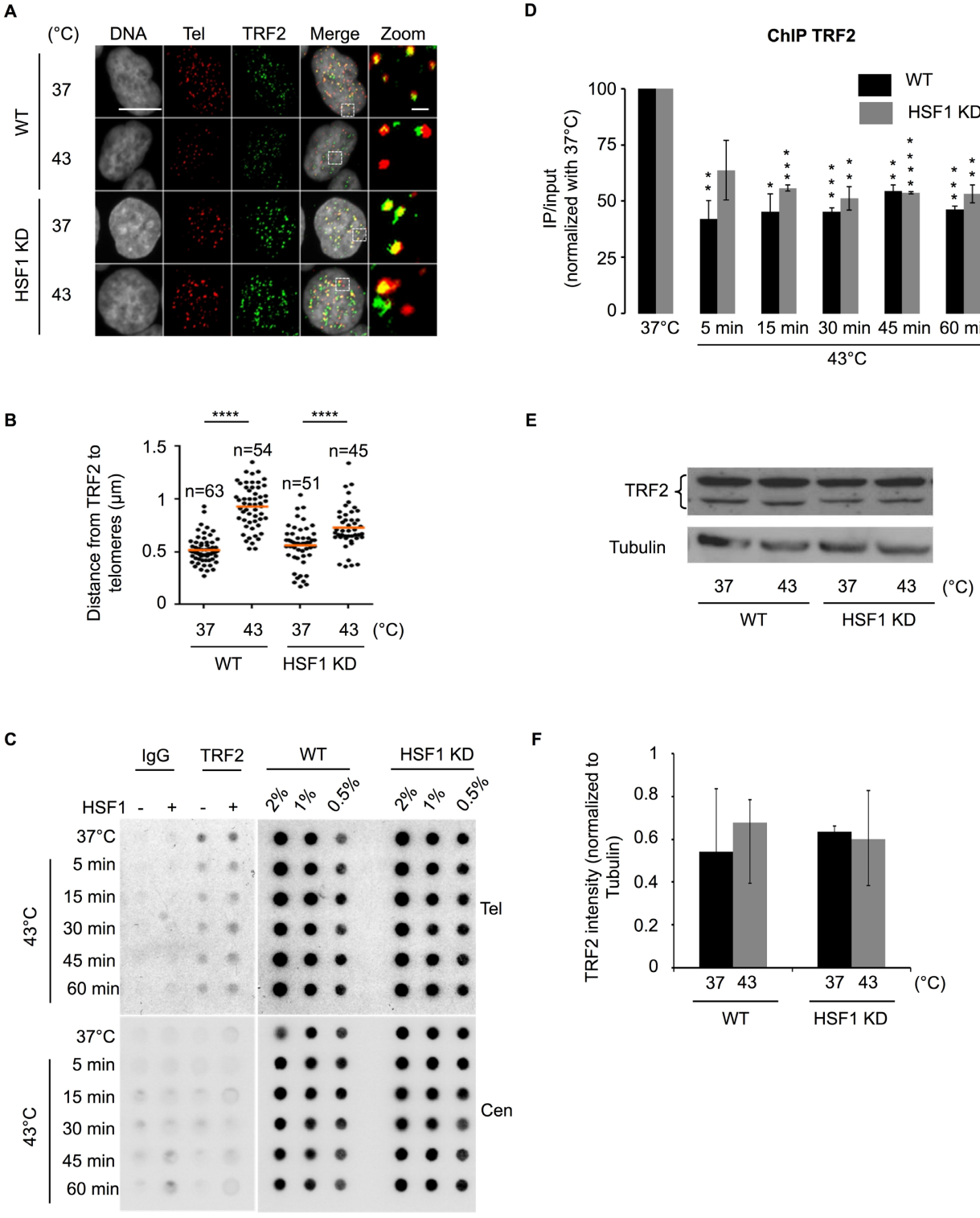

Figure 4. Heat shock induces a partial delocalization of TRF2 from telomeres. (**A**) Representative images of co-localization between telomeres detected by DNA FISH with a Cy3-$(TTACCC)_3$ probe (red) and TRF2 (green) detected by immunofluorescence in WT and HSF1 KD cells. DNA is stained with DAPI (gray). Scale bars: 100 µm (left) and 1 µm (right). (**B**) Analysis of the minimum distance in µm between TRF2 and telomeres using volocity program before and after HS. The *P*-values were calculated by unpaired Student's *t*-test with Welch's corrections and are <0.0001 for WT and HSF1 KD cells. (**C**) Dot blot of TRF2 chromatin immunoprecipitation (ChIP) analysis. ChiP experiments were performed on WT and HSF1 KD cell extracts before HS and during a kinetic of HS exposure. The blot was hybridized with radioactive telomeric and centromeric probes. Dot blot of IgG-ChIP DNA is shown as a control of specificity. (**D**) Quantification of TRF2 telomeric enrichment in ChIP experiment. Data are normalized with Input and non heat-shocked conditions. SD is based on two independent experiments. The *P*-value was calculated by unpaired Student's *t*-test with Welch's corrections. (**E**) Western blot analysis of global TRF2 expression in WT and HSF1 KD cells before and after HS. Tubulin is used as a loading control. (**F**) Quantification of global TRF2 expression before and after HS in WT and HSF1 KD cells. SD is based on two independent experiments.

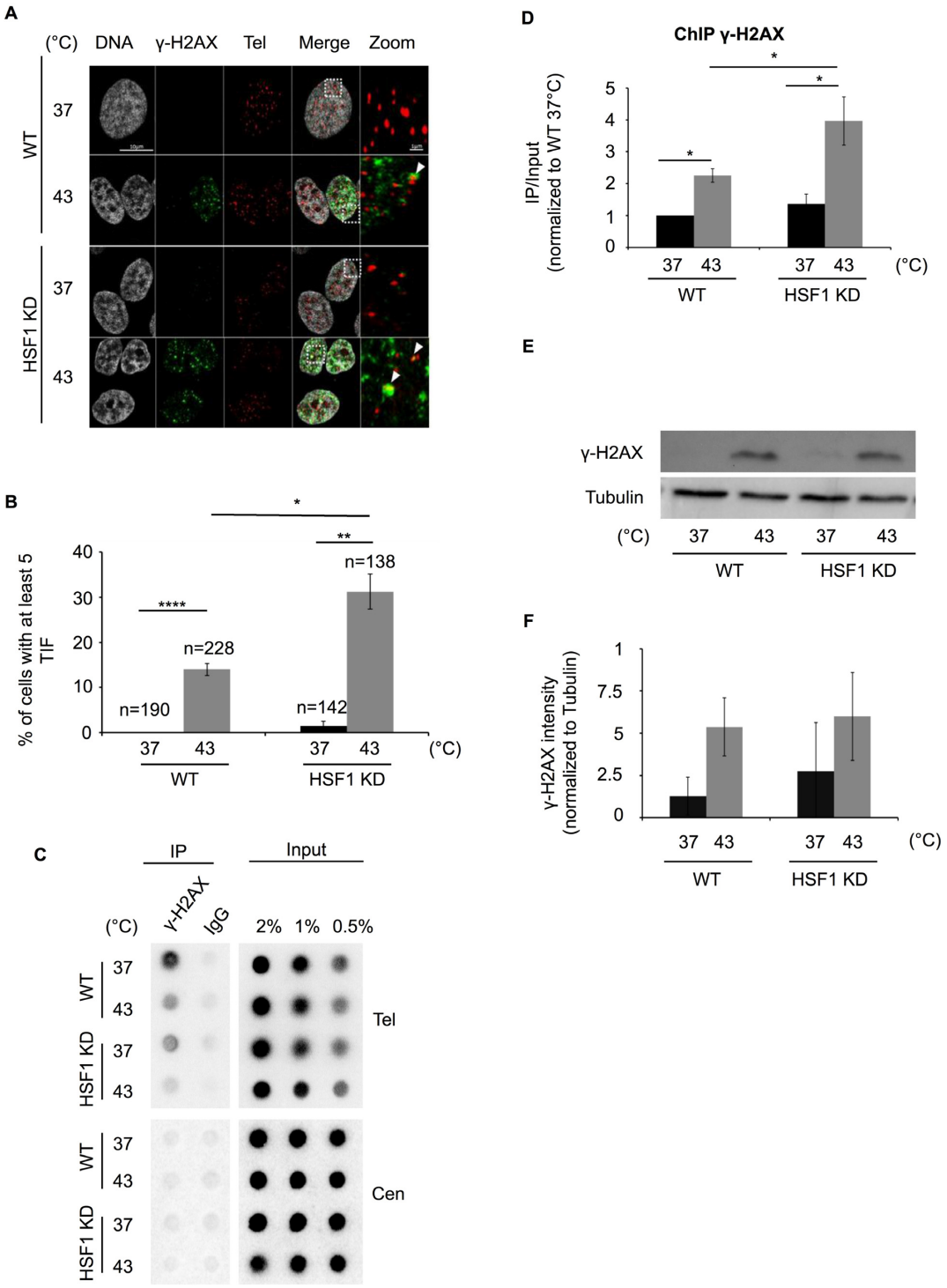

Figure 5. HSF1 helps maintaining telomere integrity upon heat shock. (**A**) Representative images of γ-H2AX foci (green) combined with DNA FISH for telomeres with a Cy3-$(TTACCC)_3$ probe (red) in WT and HSF1 KD cell before and after HS. DAPI stain is in gray. Scale bars: 100 μm (left) and 1 μm (right). (**B**) Quantification of the percentage of cells with at least five TIFs in WT and HSF1 KD cells before and after HS. The *P*-values were calculated by unpaired Student's *t*-test with Welch's corrections and are <0.0001 between 37°C and 43°C conditions for WT, 0.0019 between 37°C and 43°C for HSF1 KD and 0.0134 between WT and HSF1 KD at 43°C. (**C**) Dot blot of γ-H2AX chromatin immunoprecipitation (ChIP) analysis. ChiP experiments were performed on WT and HSF1 KD cell extracts before and after HS. The blot was hybridized with radioactive telomeric and centromeric probes. Dot blot of immunoprecipitated DNA with IgG DNA is shown as a control of specificity. (**D**) Quantification of γ-H2AX telomeric enrichment in ChIP experiments. Data are successively normalized with input and values obtained in control unstressed cells. SD deviation is based on three independent experiments. The *P*-values were calculated by unpaired Student's *t*-test with Welch's corrections and are 0.0199 between 37°C and 43°C conditions for WT, 0.0221 between 37°C and 43°C for HSF1 KD and 0.0458 between WT and HSF1 KD at 43°C. (**E**) Western blot analysis of γ-H2AX expression in WT and HSF1 KD cells before and after HS. Tubulin is shown as a loading control. (**F**) Quantification of γ-H2AX expression from western blot analysis in WT and HSF1 KD cells before and after HS. SD is based on three independent experiments.

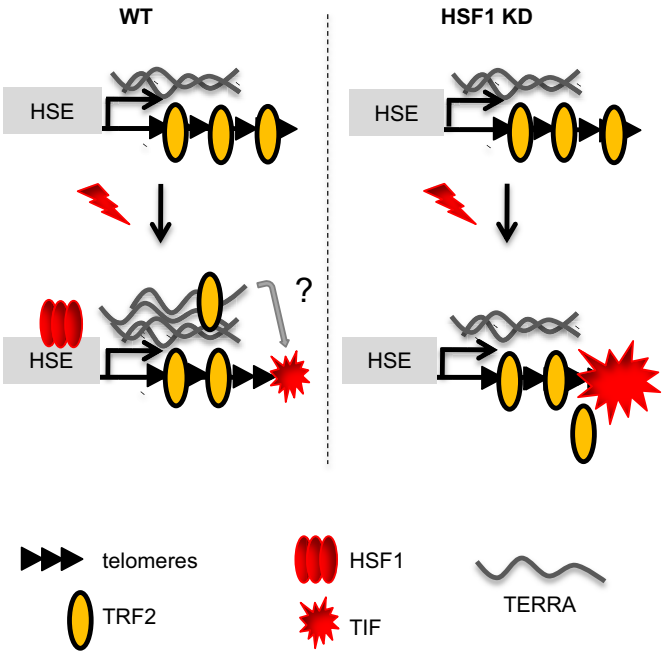

Figure 6. Possible role of HSF1 at telomeres upon HS. Heat shock induces a partial TRF2 dissociation from telomeres and the formation of telomeric dysfunction-induced foci (TIF). Upon stress, active HSF1 binds to HSE-containing subtelomeric regions and activates telomere transcription via RNAPII. Less numerous but bigger nuclear TERRA foci form in heat-shocked cells and are more associated with chromatin suggesting a possible role of TERRA in the maintenance of TRF2 at telomeric regions. In contrast, HS does not upregulate TERRA in HSF1 KD cells, and higher levels of telomeric DNA damages are observed.

this paper, we identify subtelomeric DNA as a new target of HSF1 and extend the role of HSF1 to the maintenance of telomere integrity. We show that, upon stress, HSF1 binds to telomeres to trigger TERRA accumulation and protects the telomeres from the accumulation of TIF caused by stress exposure.

We show that HSF1 is directly involved in the stress-induced up-regulation of TERRA, and demonstrate that HSF1 binding to subtelomeres promotes TERRA transcription initiated at these regions, and is restricted to telomeres containing HSEs. This analysis is therefore complementary to the analysis performed by Lingner's laboratory (11) who identified HSE within TERRA proximal promoters on seven chromosome ends (considering a 1 kb window around TERRA proximal 5′ end), as well as within 80% of TERRA proximal transcription start sites identified by RNA-Seq analysis.

Importantly, we find that HSF1 knock-down has no impact on the constitutive level of TERRA expression, suggesting that the role of HSF1 on the transcriptional activation of telomeric regions is restricted to stressed cells. To our knowledge, HSF1 is the first transcription factor identified that has a direct role in the accumulation of TERRA upon stress. The HSF1-dependent 1.8-fold induction of TERRA which we observed in stressed cells is consistent with other observations made on mouse and human cells, in which heat shock-induction rates of 1.5–2 have also been reported (8,35). The up-regulation of TERRA is not merely a consequence of the impact of stress on cell cycle progression. Indeed, only TERRA from HSE-containing telomeres are enriched with elongating RNAPII and selectively upregulated in a HSF1 dependent manner. Our data show that, upon stress, TERRA transcripts accumulate in a HSF1-dependent manner to form large nuclear foci. Interestingly, large TERRA nuclear foci were also identified in proliferating mouse cerebellar neuronal progenitors and medulloblastoma as a consequence of a high level of TERRA expression (36). These foci have been proposed to represent new nuclear bodies with still unknown functions. In human cells, a fraction of telomeric RNAs also resides within the nucleoplasm (37), suggesting that TERRA molecules would not be constitutively associated with telomeres. In heat-shocked cells, we find that the total number of TERRA foci per nucleus slightly decreases, whereas, in contrast, no clustering of telomeres was observed by DNA FISH, suggesting that a specific stress-induced clustering of TERRA occurs. Since a study has demonstrated that TERRA transcripts from a single telomere could associate with multiple chromosome ends (38), our data suggest that TERRA may diffuse from their sites of transcription to accumulate as foci outside telomeres or at other telomeres. Alternatively, the possibility of a shut-down of transcription involving only certain telomeres cannot be excluded. Further investigation on TERRA dynamics will be necessary to better understand TERRA mobility upon stress.

HS has also been shown to impact DNA replication (39) and to specifically inhibit homologous recombination (HR) involved in both DNA repair (40) and formation of telomere-specific structures. Here, we bring evidence that HS impacts telomere capping in the different cell lines analyzed. We find that TRF2 partially dissociates from telomeres already after 5 min of HS in both WT and HSF1 KD cells, whereas, in contrast, TERRA upregulation is only observed after 30 min of stress exposure, demonstrating that TRF2 displacement from telomeres takes place before TERRA upregulation and is therefore independent on this upregulation. Heat shocked-induced partial TRF2 dissociation may result from structural alterations affecting TRF2 or TRF2 partners. Moreover, TRF2 is known to repress TERRA transcription through its homodimerization domain and to induce heterochromatin compaction (11). In agreement with what has already been reported in the literature (11), we find that TERRA is overexpressed in TRF2 KD cells as compared to HS WT cells (Supplementary Figure S2C). In stressed or unstressed cells TRF2 KD cells, HSF1 has no impact on TERRA expression. Together these data indicate that under HS, where TRF2 only partially dissociates from telomeres, HSF1 is required for proper upregulation of TERRA in WT cells (Supplementary Figure S2D).

We also find that HS impacts telomere integrity in WT and HSF1 KD cells using TRF2 as a marker of telomere capping and γH2AX as a marker of DNA damage. These observations do not corroborate with the data from Petrova *et al.* (34) showing that heat shock triggers a total loss of TRF2 foci with no increase of γH2AX at telomeres. This discrepancy may be due to the differences in the conditions used for stress (respectively 43°C and 45°C) between the two studies, respectively typified in the literature

as mild and severe HS, which induce different cellular response (41). Moreover, in our conditions, TRF2 still forms foci after heat shock, suggesting that at least part of TRF2 remains localized in close proximity to telomeres. This is in agreement with previous studies (24,42,43). Interestingly, our data show an enrichment of nuclear TERRA associated with chromatin in response to heat stress (Supplementary Figure S4). Since TERRA interacts directly with TRF2 (20), it is possible upon heat shock, that part of TRF2 protein that dissociates from telomeres, remains in close proximity to telomeres thanks to its interaction with chromatin-bound TERRA molecules. The DNA damages we observe at telomeres upon HS may result in part from partial telomeres uncapping. A causal relationship between TRF2 delocalization from telomeres and the induction of telomere damages has already been described (44). However, our results suggest that partial TRF2 dissociation from telomeres cannot be the only cause of telomeric damages in stressed cells. Indeed, the same ratio of TRF2 dissociation from telomeres is observed in both WT and HSF1 KD cells, whereas the number of cells with TIF drastically increases in HSF1 KD cells compared to WT cells. Likewise, we cannot exclude that stress-induced chromatin conformation changes at telomeres also impact on the efficacy of the DNA repair machinery. Finally, the presence of TIF may also reveal the existence of a small number of replication fork arrests, since γH2AX is also thought to protect stress-induced arrested replication forks (39). Whatever the exact mechanisms underlying the formation of TIF in heat-shocked cells are, the presence of TIF, correlating with partial TRF2 uncapping at telomeres, suggests that HS both impacts on both telomere capping and telomere integrity.

Interestingly, we find that HSF1 plays a role in telomere protection upon stress. Indeed, we show that HS triggers more DNA damages in HSF1 KD cells than in WT cells, suggesting a more effective DNA damage response (DDR) in WT cells in the early telomeric response. However, we cannot exclude the presence of lower amounts of stress-induced DNA damages in WT cells than in HSF1 KD cells. A rapid HSF1-dependent accumulation of TERRA may protect telomeres by participating to the DDR, triggered by dysfunctional telomeres. Upregulation of TERRA may promote the synergistic effect of telomere end processing and chromatin remodeling factors at telomeres. Porro and colleagues (11) indeed showed that TERRA upregulation correlates with the telomeric recruitment of the lysine-specific demethylase (LSD1). LSD1 directly interacts with TERRA and Mre11, a subunit of the MRE11/RAD50/NBS1 (MRN) complex required for the resection of the telomeric 3′ overhang and this may promote chromosome fusion at dysfunctional telomeres. TERRA transcripts can also promote changes in chromatin structure of uncapped telomeres facilitating end fusions of TRF2-depleted telomeres (11). Another possibility is that TERRA may preserve telomeric higher-order structure upon heat shock. A functional link between TERRA induction and chromatin reorganization of dysfunctional telomeres has been proposed (11). Moreover, TERRA has been implicated in the deposition of H3K9me3 at functional telomeres (20). TERRA enrichment in the chromatin fraction after heat shock suggests it may play a direct role in the maintenance and/or formation of heterochromatin upon heat stress making telomeric chromatin less accessible to DNA damages.

In addition, based on the new emerging concept that RNAs may play a role as thermosensors (45), TERRA may transduce the stress signal to essential actors with other important roles in the stress response. Moreover, our results show that the role of HSF1 in telomeric protection is restricted to the early stage of the stress response.

An intriguing question is why HSE are only present at certain chromosomes and consequently, why an up regulation of TERRA transcripts only occurs at a particular subset of chromosomes. A possible hypothesis is that HSF1-upregulated TERRA could diffuse from their sites of transcription and act in *trans* to protect telomeres and/or to promote chromatin remodeling at telomeres. Interestingly, in mouse and yeast, TERRA are not expressed from all telomeres at a given time and TERRA produced at a specific locus are able to relocate at different telomeres (18,38).

To conclude, HSF1 appears as a new transcription factor of TERRA, and as an essential actor to protect telomeres upon stress (Figure 6). Based on our results and given the important role of HSF1 in tumor formation (46) and telomere biology, defining the exact role of HSF1 with regard to telomere stability in tumor development already emerges as a promising field of research.

SUPPLEMENTARY DATA

Supplementary Data are available at NAR Online.

ACKNOWLEDGEMENTS

The authors thank Dr L. Sistonen (University of Turku, Finland) for the gift of wild type and knocked-down HeLa cells for HSF1. We also thank Dr Eric Gilson, Dr Vincent Géli and Dr Mary Callanan for fruitful discussions and Dr Sophie Green for her critical reading of the manuscript. We thank all the members of the microscopy platform of IAB. This work was funded by 'Ligue contre le cancer' and by Grenoble Alpes University grants.

FUNDING

Ligue Contre le cancer [R13FAURE, R14FAURE]; Grenoble Alpes University. Funding for open access charge: Institut national de la santé et de la recherche médicale.
Conflict of interest statement. None declared.

REFERENCES

1. Ritossa,F. (1962) A new puffing pattern induced by temperature shock and DNP in drosophila. *Experientia*, **18**, 571–573.
2. Audas,T.E. and Lee,S. (2015) Stressing out over long noncoding RNA. *Biochim. Biophys. Acta*, **1859**, 184–191.
3. Akerfelt,M., Morimoto,R.I. and Sistonen,L. (2010) Heat shock factors: integrators of cell stress, development and lifespan. *Nat. Rev. Mol. Cell Biol.*, **11**, 545–555.
4. Jolly,C., Metz,A., Govin,J., Vigneron,M., Turner,B.M., Khochbin,S. and Vourc'h,C. (2004) Stress-induced transcription of satellite III repeats. *J. Cell Biol.*, **164**, 25–33.
5. Metz,A., Soret,J., Vourc'h,C., Tazi,J. and Jolly,C. (2004) A key role for stress-induced satellite III transcripts in the relocalization of splicing factors into nuclear stress granules. *J. Cell Sci.*, **111**, 4551–4558.

6. Biamonti,G. and Vourc'h,C. (2010) Nuclear stress bodies. *Cold Spring Harbor Perspect. Biol.*, **2**, 1–12.
7. Blasco,M. and Schoeftner,S. (2008) Developmentally regulated transcription of mammalian telomeres by DNA-dependent RNA polymerase II. *Nat. Cell Biol.*, **10**, 228–236.
8. Eymery,A., Horard,B., el Atifi-Borel,M., Fourel,G., Berger,F., Vitte,A.L., Van den Broeck,A., Brambilla,E., Fournier,A., Callanan,M. *et al.* (2009) A transcriptomic analysis of human centromeric and pericentric sequences in normal and tumor cells. *Nucleic Acids Res.*, **37**, 6340–6354.
9. Romano,G.H., Harari,Y., Yehuda,T., Podhorzer,A., Rubinstein,L., Shamir,R., Gottlieb,A., Silberberg,Y., Pe'er,D., Ruppin,E. *et al.* (2013) Environmental stresses disrupt telomere length homeostasis. *PLoS Genet.*, **9**, 1–9.
10. De Lange,T. (2005) Shelterin: The protein complex that shapes and safeguards human telomeres. *Genes Dev.*, **19**, 2100–2110.
11. Porro,A., Feuerhahn,S., Delafontaine,J., Riethman,H., Rougemont,J. and Lingner,J. (2014) Functional characterization of the TERRA transcriptome at damaged telomeres. *Nat. Commun.*, **5**, 5379.
12. Azzalin,C.M., Reichenbach,P., Khoriauli,L., Giulotto,E. and Lingner,J. (2007) Telomeric repeat containing RNA and RNA surveillance factors at mammalian chromosome ends. *Science (New York, N.Y.)*, **318**, 798–801.
13. Nergadze,S.G., Farnung,B.O., Wischnewski,H., Khoriauli,L., Vitelli,V., Chawla,R., Giulotto,E. and Azzalin,C.M. (2009) CpG-island promoters drive transcription of human telomeres. *RNA (New York, N.Y.)*, **15**, 2186–2194.
14. Yehezkel,S., Segev,Y., Viegas-Péquignot,E., Skorecki,K. and Selig,S. (2008) Hypomethylation of subtelomeric regions in ICF syndrome is associated with abnormally short telomeres and enhanced transcription from telomeric regions. *Hum. Mol. Genet.*, **17**, 2776–2789.
15. Arnoult,N., Van Beneden,A. and Decottignies,A. (2012) Telomere length regulates TERRA levels through increased trimethylation of telomeric H3K9 and HP1α;. *Nat. Struct. Mol. Biol.*, **19**, 948–956.
16. Caslini,C., Connelly,J.A., Serna,A., Broccoli,D. and Hess,J.L. (2009) MLL associates with telomeres and regulates telomeric repeat-containing RNA transcription. *Mol. Cell. Biol.*, **29**, 4519–4526.
17. Redon,S., Reichenbach,P. and Lingner,J. (2010) The non-coding RNA TERRA is a natural ligand and direct inhibitor of human telomerase. *Nucleic Acids Res.*, **38**, 5797–5806.
18. Cusanelli,E., Romero,C.A.P. and Chartrand,P. (2013) Telomeric noncoding RNA TERRA is induced by telomere shortening to nucleate telomerase molecules at short telomeres. *Mol. Cell*, **51**, 780–791.
19. Moravec,M., Wischnewski,H., Bah,A., Hu,Y., Liu,N., Lafranchi,L., King,M.C. and Azzalin,C.M. (2016) TERRA promotes telomerase-mediated telomere elongation in Schizosaccharomyces pombe. *EMBO Rep.*, **7**, 999–1012.
20. Deng,Z., Norseen,J., Wiedmer,A., Riethman,H. and Paul,M. (2009) TERRA RNA Binding to TRF2 facilitates heterochromatin formation and ORC recruitment at telomeres. *Mol. Cell*, **35**, 403–413.
21. Flynn,R.L., Centore,R.C., O'Sullivan,R.J., Rai,R., Tse,A., Songyang,Z., Chang,S., Karlseder,J. and Zou,L. (2011) TERRA and hnRNPA1 orchestrate an RPA-to-POT1 switch on telomeric single-stranded DNA. *Nature*, **471**, 532–536.
22. Maeda,T., Guan,J.-Z., Koyanagi,M. and Makino,N. (2013) Alterations in the telomere length distribution and the subtelomeric methylation status in human vascular endothelial cells under elevated temperature in culture condition. *Aging Clin. Exp. Res.*, **25**, 231–238.
23. Martínez-Guitarte,J.L., Díez,J.L. and Morcillo,G. (2008) Transcription and activation under environmental stress of the complex telomeric repeats of Chironomus thummi. *Chromosome Res.*, **16**, 1085–1096.
24. Deng,Z., Wang,Z., Stong,N., Plasschaert,R., Moczan,A., Chen,H.-S., Hu,S., Wikramasinghe,P., Davuluri,R.V., Bartolomei,M.S. *et al.* (2012) A role for CTCF and cohesin in subtelomere chromatin organization, TERRA transcription, and telomere end protection. *EMBO J.*, **31**, 4165–4178.
25. Pernet,L., Faure,V., Gilquin,B., Dufour-Guérin,S., Khochbin,S. and Vourc'h,C. (2014) HDAC6-ubiquitin interaction controls the duration of HSF1 activation after heat shock. *Mol. Biol. Cell*, **25**, 4187–4194.
26. Stong,N., Deng,Z., Gupta,R., Paul,S., Eichler,E.E., Graves,T., Fronick,C.C., Courtney,L., Wilson,R.K., Lieberman,P. *et al.* (2014) Subtelomeric CTCF/Cohesin binding site organization using improved subtelomere assemblies and novel annotations. *Genome Res.*, **6**, 1039–1050.
27. Amin,J., Ananthan,J. and Voellmy,R. (1988) Key features of heat shock regulatory elements. *Mol. Cell. Biol.*, **8**, 3761–3769.
28. Pelham,H.R. (1982) A regulatory upstream promoter element in the Drosophila hsp 70 heat-shock gene. *Cell*, **30**, 517–528.
29. Sorger,P.K. and Pelham,H.R. (1988) Yeast heat shock factor is an essential DNA-binding protein that exhibits temperature-dependent phosphorylation. *Cell*, **54**, 855–864.
30. Perisic,O., Xiao,H. and Lis,J.T. (1989) Stable binding of Drosophila heat shock factor to head-to-head and tail-to-tail repeats of a conserved 5 bp recognition unit. *Cell*, **59**, 797–806.
31. Sorger,P.K. (1991) Heat shock factor and the heat shock response. *Cell*, **65**, 363–366.
32. Selth,L.A., Sigurdsson,S. and Svejstrup,J.Q. (2010) Transcript Elongation by RNA Polymerase II. *Annu. Rev. Biochem.*, **79**, 271–293.
33. Nechaev,S. and Adelman,K. (2011) Pol II waiting in the starting gates: Regulating the transition from transcription initiation into productive elongation. *Biochim. Biophys. Acta - Gene Regul. Mech.*, **1809**, 34–45.
34. Petrova,N.V., Velichko,A.K., Kantidze,O.L. and Razin,S.V. (2014) Heat shock-induced dissociation of TRF2 from telomeres does not initiate a telomere-dependent DNA damage response. *Cell Biol. Int.*, **38**, 675–681.
35. López de Silanes,I., Stagno d'Alcontres,M. and Blasco,M.A. (2010) TERRA transcripts are bound by a complex array of RNA-binding proteins. *Nat. Commun.*, **1**, 33.
36. Deng,Z., Wang,Z., Xiang,C., Molczan,A., Baubet,V., Conejo-Garcia,J., Xu,X., Lieberman,P.M. and Dahmane,N. (2012) Formation of telomeric repeat-containing RNA (TERRA) foci in highly proliferating mouse cerebellar neuronal progenitors and medulloblastoma. *J. Cell Sci.*, **125**, 4383–4394.
37. Porro,A., Feuerhahn,S., Reichenbach,P. and Lingner,J. (2010) Molecular dissection of telomeric repeat-containing RNA biogenesis unveils the presence of distinct and multiple regulatory pathways. *Mol. Cell. Biol.*, **30**, 4808–4817.
38. Lopez de Silanes,I., Grana,O., De Bonis,M.L., Dominguez,O., Pisano,D.G. and Blasco,M.A. (2014) Identification of TERRA locus unveils a telomere protection role through association to nearly all chromosomes. *Nat. Commun.*, **5**, 4723.
39. Velichko,A.K., Petrova,N.V., Kantidze,O.L. and Razin,S.V. (2012) Dual effect of heat shock on DNA replication and genome integrity. *Mol. Biol. Cell*, **23**, 3450–3460.
40. Krawczyk,P.M., Eppink,B., Essers,J., Stap,J., Rodermond,H., Odijk,H., Zelensky,A., van Bree,C., Stalpers,L.J., Buist,M.R. *et al.* (2011) Mild hyperthermia inhibits homologous recombination, induces BRCA2 degradation, and sensitizes cancer cells to poly (ADP-ribose) polymerase-1 inhibition. *Proc. Natl. Acad. Sci. U.S.A.*, **108**, 9851–9856.
41. Tanabe,M., Nakai,A., Kawazoe,Y. and Nagata,Y. (1997) Different thresholds in the responses of two heat shock transcription factors, HSF1 and HSF3. *J. Biol. Chem.*, **272**, 15389–15395.
42. Madlener,S., Ströbel,T., Vose,S., Saydam,O., Price,B.D., Demple,B. and Saydam,N. (2013) Essential role for mammalian apurinic/apyrimidinic (AP) endonuclease Ape1/Ref-1 in telomere maintenance. *Proc. Natl. Acad. Sci. U.S.A.*, **110**, 17844–17849.
43. Simonet,T., Zaragosi,L.E., Philippe,C., Lebrigand,K., Schouteden,C., Augereau,A., Bauwens,S., Ye,J., Santagostino,M., Giulotto,E. *et al.* (2011) The human TTAGGG repeat factors 1 and 2 bind to a subset of interstitial telomeric sequences and satellite repeats. *Cell Res.*, **21**, 1028–1038.
44. Zhou,W.J., Deng,R., Zhang,X.Y., Feng,G.K., Gu,L.Q. and Zhu,X.F. (2009) G-quadruplex ligand SYUIQ-5 induces autophagy by telomere damage and TRF2 delocalization in cancer cells. *Mol. Cancer Ther.*, **8**, 3203–3213.
45. Shamovsky,I., Ivannikov,M., Kandel,E.S., Gershon,D. and Nudler,E. (2006) RNA-mediated response to heat shock in mammalian cells. *Nature*, **440**, 556–560.
46. Dai,C., Whitesell,L., Rogers,A.B. and Lindquist,S. (2007) Heat shock factor 1 is a powerful multifaceted modifier of carcinogenesis. *Cell*, **130**, 1005–1018.